

Enhanced Aluminum reflecting and solar-blind filter coatings for the far-ultraviolet

Javier Del Hoyo* and Manuel Quijada

NASA Goddard Space Flight Center, 8800 Greenbelt Road, Greenbelt, Maryland 20771, USA

*javier.delhoyo@nasa.gov

ABSTRACT

The advancement of far-ultraviolet (FUV) coatings is essential to meet the specified throughput requirements of the Large UV/Optical/IR (LUVOIR) Surveyor Observatory which will cover wavelengths down to the 100 nm range. The biggest constraint in the optical thin film coating design is attenuation in the Lyman-Alpha Ultraviolet range of 100-130 nm in which conventionally deposited thin film materials used in this spectral region (e.g. aluminum [Al] protected with Magnesium fluoride [MgF₂]) often have high absorption and scatter properties degrading the throughput in an optical system. We investigate the use of optimally deposited aluminum and aluminum tri-fluoride (AlF₃) materials for reflecting and solar blind band-pass filter coatings for use in the FUV. Optical characterization of the deposited designs has been performed using UV spectrometry. The optical thin film design and optimal deposition conditions to produce superior reflectance and transmittance using Al and AlF₃ are presented.

Keywords: aluminum tri-fluoride, AlF₃, aluminum, Al, Fabry-Perot type filter, ultraviolet, FUV, dielectric metal filter, metal fluoride, band-pass filter, broadband.

1. INTRODUCTION

The Large Ultra-Violet/Optical/Infrared (LUVOIR) Surveyor is a large mission concept study announced by the NASA Astrophysics Division in 2016 that will allow for a plethora of scientific observations.¹ In order to achieve these scientific objectives, the design will consist of a core telescope design that will be directing photons into instruments covering each respective spectral channel. Dissimilar to prior NASA flagship missions such as the Hubble Space Telescope (HST), the LUVOIR surveyor UV channel aims to capture the entirety of the Lyman-ultraviolet (LUV) spectral band (i.e. 91.2 nm - 121.6 nm) with a stretch goal of covering the ~90 nm - 300 nm range.² The LUV spectral band is a highly desirable band in the astrophysics community due to its large spectroscopic line density.³

To understand the importance of thin film coatings, we can analyze the number of spectral photons going through an optical system and detector by considering the spectral radiant flux give as:^{4,5}

$$\Phi_{\lambda} = L_{\lambda} \cdot A_{EP} \cdot \Omega, \quad (1)$$

where λ is the wavelength under observation, Φ_{λ} is the spectral radiant flux, L_{λ} is the spectral radiance of the object or source at a chosen wavelength, A_{EP} is the area of the entrance pupil, and Ω is the solid angle defined by the diameter and focal length of the imaging mirror. A baseline imaging spectrograph design is composed of a core Cassegrain telescope with a slit at the intermediate image/focal plane followed by a concave grating serving as both the dispersive and imaging element.⁶ The spectral radiant flux in Joules for a spatially resolved spectroscopic observation will then be given as:

$$\Phi_{\lambda} = \tau_{\lambda} \cdot L_{\lambda} \cdot A_{EP} \cdot \Omega \cdot R_{\lambda, optics} \cdot \epsilon_{\lambda, grat.} \cdot Q_{\lambda, det.} \cdot \Delta\lambda \cdot \Delta t, \quad (2)$$

where τ_{λ} is the spectral transmission through the media of light propagation, $R_{\lambda, optics}$ is the total reflectance of the optics, $\epsilon_{\lambda, grat.}$ is the grating efficiency, $Q_{\lambda, det.}$ is the detector efficiency, $\Delta\lambda$ is the spectral bandwidth across the detector area, and Δt is the integration time. (Note: There are sources of uncertainty such as polarization and scattered light not considered in this equation).

It is exceptionally critical to increase the spectral radiant flux in the ultraviolet range since the smaller wavelengths are more subject to scatter and absorption traveling from an interstellar medium and through an optical system. Common techniques used to increase this value include designing the spectroscopic system so most of the optical elements are reflective, limiting the number of optical elements, and increasing the integration time. These methods, however, limit instrument design freedom and increasing integration time often leads to unwanted noise and compromises observational data. Therefore, it is imperative that high performance coatings be developed as the coatings can improve the total reflectance of the optics, the grating efficiency, as well as the detector efficiency.

In this paper, we present Al and AlF_3 reflector and metal-dielectric Fabry-Perot type filter FUV coating design data which can be used in future LUVOIR instrument design. Technical background and our approach to choosing the materials for the broadband reflector and UV filter design is shown in Section 2. The thin film deposition method and measurement method is described in Section 3. The results and concluding remarks are respectively given in Sections 4 and 5.

2. BROADBAND COATINGS AND UV BAND-PASS FILTER DESIGN

In order to meet the ultraviolet to infrared specifications, the core telescope will require a broadband coating covering the UV to infrared spectral ranges while the secondary instruments will contain coatings optimizing each respective channel while attenuating others. There are a variety of materials for thin film reflector and filter coating design in the visible and infrared spectral ranges, but the amount of materials that will limit photon loss in the deep ultraviolet below ~ 120 nm is extremely limited.⁷ Therefore, the band-pass filters in this study will be designed for the UV.

2.1. Reflecting broadband coatings

Pure Al is the most prominent material to be used as a broadband reflector as it performs well from the UV to IR spectral ranges.⁸ However, it becomes oxidized following thin film deposition causing its FUV properties to severely degrade, thus it requires a thin overcoat of a transmissive protection layer to serve as a protection barrier as well as enhance its UV performance due to interference effects.^{9,10} Thin metal fluoride overcoats (i.e. \sim quarter wave) of MgF_2 or lithium fluoride (LiF) on aluminum are often used for UV applications since these materials have a high bandgap energy and a low cut off / absorption wavelength.¹¹

The optical properties of these metal fluorides have recently been advanced as highly dense and reflective protected aluminum coatings with an intrinsic cut-off wavelength closer to the theoretical limit were developed using physical vapor deposition (PVD) and substrate heating.¹² However, the MgF_2 cut-off wavelength is near 115 nm while LiF is extremely hygroscopic leading to FUV optical property degradation over time.^{12,13} Therefore, it is necessary to find a more robust overcoat material with a smaller cut-off wavelength in order to meet LUVOIR coating requirements. AlF_3 and MgF_2 have been shown to have similar bandgap energy,¹⁴ so it is a viable replacement as a protective overcoat on aluminum.

2.2. Fabry-Perot type band-pass filter design

The use of a metal-dielectric Fabry-Perot type band-pass filter composed of a thin layer of aluminum and a metal-fluoride could be used to suppress any unwanted photons from the visible spectrum and separate overlapping orders by the grating in the spectroscopic system. The Fabry-Perot type filter is based on the Fabry-Perot etalon, however, instead of an air gap between the reflective surfaces, a dielectric is substituted as a spacer layer.⁷ The Fabry-Perot filter works on the basis of the waves of reflected light from the successive interfaces of the cavity adding up out of phase and destructively interfering, causing only a certain wavelength or spectral band to transmit. Usually, the number of cavities (i.e. metal, dielectric, metal) is increased in filter design to increase the steepness of the band-pass edge cut-offs to more optimally attenuate unwanted wavelengths, and an extra dielectric layer is added over the final metal layer to prevent oxidation.^{7,15} The study of these filters in the UV has performed in prior publications, however, the filter performance has not been validated below ~ 175 nm.¹⁵⁻¹⁷

Al and AlF_3 are excellent candidates for the design of a metal, dielectric, metal, dielectric filters for the reasons stated above. The thin layer of Al will be used to suppress visible light while the low UV absorption properties of AlF_3 will be used to optimize an FUV band-pass. Figure 1 shows the proposed Fabry-Perot type band-pass filter design using a MgF_2

substrate with Al as the metal layer and AlF_3 as the dielectric layer. The number of layers is kept at a minimum to prevent absorption losses in the FUV and MgF_2 is chosen as the substrate since it is the least hygroscopic/ hydrophilic metal fluoride with proven space flight heritage.¹⁸

Aluminum tri-fluoride
Aluminum
Aluminum tri-fluoride
Aluminum
Magnesium Fluoride

Figure 1. Metal dielectric Fabry-Perot type filter design using aluminum as the metal and aluminum tri-fluoride as the dielectric spacer layer deposited on a thin magnesium fluoride substrate.

3. MATERIAL DEPOSITION AND OPTICAL CHARACTERIZATION

3.1 Physical vapor deposition

High power thermal resistive evaporation in an ultra-high vacuum chamber was used to deposit the Al and AlF_3 materials. High purity Al staples were wrapped around tungsten filaments while the AlF_3 was placed into a molybdenum resistive bowl. The chamber was pumped to $<1 \times 10^{-7}$ torr before the process was started. Quartz crystal monitors were used to monitor the deposited material thickness and rate while high speed shutters over the depositing sources were used to control the final deposited thickness.

The three-step thermal resistive evaporation process is utilized for the deposition of the Al+ AlF_3 reflecting films.¹² A 70 nm thin film of Al was deposited onto a 50 mm x 50 mm quartz substrate at ambient temperature. The process was immediately followed by a thin 4 nm film of AlF_3 as a protective layer before heating the substrate. Finally, the substrate was heated to 250°C before the final AlF_3 layer was deposited with respective thicknesses of 20.5 nm and 20.1 nm for each experimental case. The deposition parameters are summarized in Table 1.

Table 1. Deposition parameters for deposited Al and AlF_3 films

Material Layer	Deposition Method	Rate (nm/sec)	Final Layer Thickness (nm)	Deposited Material Purity %	Substrate Temperature °C
Al	Resistive Evaporation	10	70	99.999	27
AlF_3	Resistive Evaporation	2	4	99.500	27
AlF_3^*	Resistive Evaporation	3	20.5, 20.1	99.500	250

AlF_3^* denotes a different AlF_3 thickness parameter used for each respective deposition process.

To optically characterize the AlF_3 , a 24.5 nm layer of AlF_3 was deposited on a MgF_2 window which was manufactured with a cut along the optical axis to minimize birefringence.¹⁹ The substrate was heated to 250°C before the AlF_3 layer was applied. The layer was deposited using same deposition parameters outlined in the final layer of AlF_3 on Table 1.

3.2 UV and visible optical characterization of deposited coatings

The optical reflectance and transmittance measurements in the FUV spectral range were performed using a McPherson Vacuum Ultraviolet (VUV) AS 10X reflectometer. The instrument uses a hollow cathode gas purged light source to create a plasma covering the spectral lines of each respective gas fed into the source (e.g. hydrogen, neon, and helium).

Radiation from the ionized gas then enters an entrance slit into a wavelength-tuning grating which relays the dispersed radiation into an exit slit, order sorting filters, and system aperture stop before reaching the element under test. Light can be reflected or transmitted from the element under test into photomultiplier tube (PMT) where the photons are absorbed and converted into electrons. The reflectometer used for the measurements is shown in Figure 2.



Figure 2. McPherson VUV reflectometer used for extreme ultraviolet and far ultraviolet (i.e. 58.4 nm to 200 nm) reflectance and transmittance measurements.

An absolute measurement is performed by first taking a reference measurement without the element under test in the optical path of the radiation. The test element is then inserted into the optical path under transmission or reflection and a second measurement is obtained. For a transmittance measurement, the element under test is normal to the light source and PMT waveguide facet. A reflectance measurement consists of the element under test positioned at an angle of incidence of 10° while the PMT waveguide facet is rotated and angled at 20° in the optical path of the reflected light. The ratio of the radiation with the element under in the optical path over the radiation without the element under test in the optical path is then given as the respective transmittance or reflectance.

This AlF_3 film was also optically characterized at larger UV to visible wavelengths with a Perkin Elmer Lambda 950 spectrometer. This spectrometer contains various channels capable of measuring the 190 nm to 2500 nm spectral range. This would allow of further wavelength characterization in the design of the proposed band-pass filter.

To derive the optical properties of the deposited AlF_3 film, the MgF_2 window to be coated was first measured in transmission and reflection. Using these values and the known thickness, the index of refraction, $n(\lambda)$, and extinction coefficient, $k(\lambda)$, of the window were extracted using a least squares fit to the theoretical Fresnel transmittance and reflectance equations with the FilmStar program. Through several iterations, the program adjusts the index of refraction and extinction coefficients as a function of wavelength until these values agree to the measured spectral reflectance and transmittance to $\pm 1\%$. The reflectance and transmittance of the window were then re-measured after applying a quarter wave of AlF_3 optimized at 121 nm. The index of refraction and extinction coefficients of the AlF_3 layer were then extracted using a similar least squares fit with the known optical properties of the window.

4. ALUMINUM AND ALUMINUM TRI-FLUORIDE COATING RESULTS

4.1 Deposited Al and AlF_3 broadband reflectors

The viability of using AlF_3 as an overcoat over Al to replace MgF_2 and LiF as a broadband reflector was investigated in this study. The deposition parameters for depositing this coating design are outlined in Table 1 in Section 3.1. Unlike MgF_2 and LiF, when heating the AlF_3 during thermal resistive evaporation, the substance sublimates. Thus reducing any pinholes that may arise during ejection of small un-melted source particles due to the gas accumulation in the confinements of the boat during the heating process. The FUV reflectance of two deposited Al+ AlF_3 designs is shown in Figure 3.

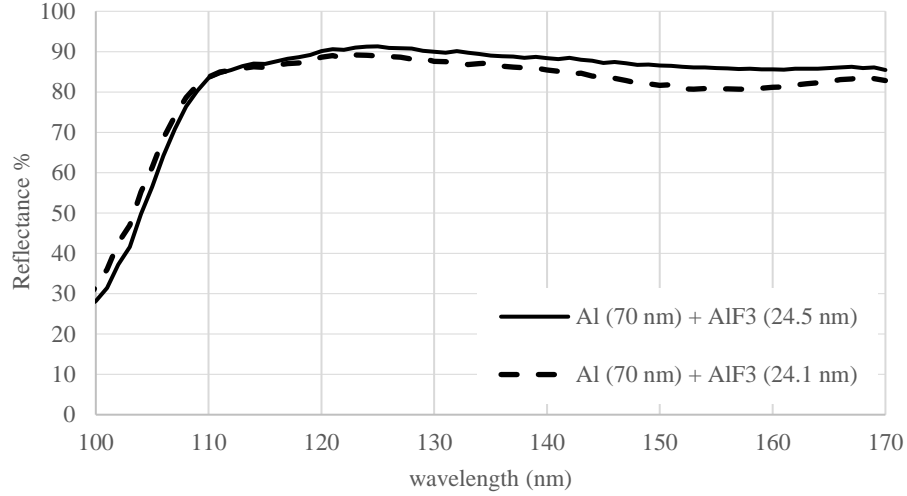


Figure 3. FUV Reflectance vs. Wavelength of deposited Al+AlF₃ samples.

It is evident that both designs produces optimal FUV reflectance results. Both designs maintained a reflectance of more than 80% from 109 to 170 nm. The first sample with an AlF₃ thickness of 24.5 nm peaked with a reflectance of 91.3% at 125 nm and maintained a high reflectance of more than 90% from 120 nm to 130 nm. The second sample with the 24.1 nm thickness peaked at Lyman-Alpha (121.6 nm) with a reflectance of 89% and maintained slightly higher reflectance at smaller wavelengths starting at 110 nm while slightly underperforming the first sample at the larger wavelengths. The slight dip after the peak wavelength is attributed to slight interference effects.

4.2 Derived AlF₃ optical properties

In order to design a suitable band-pass filter, the optical properties of the AlF₃ layer were derived as described in section 3.2. The filter has to contain high UV transmission properties with strong rejection of visible light.

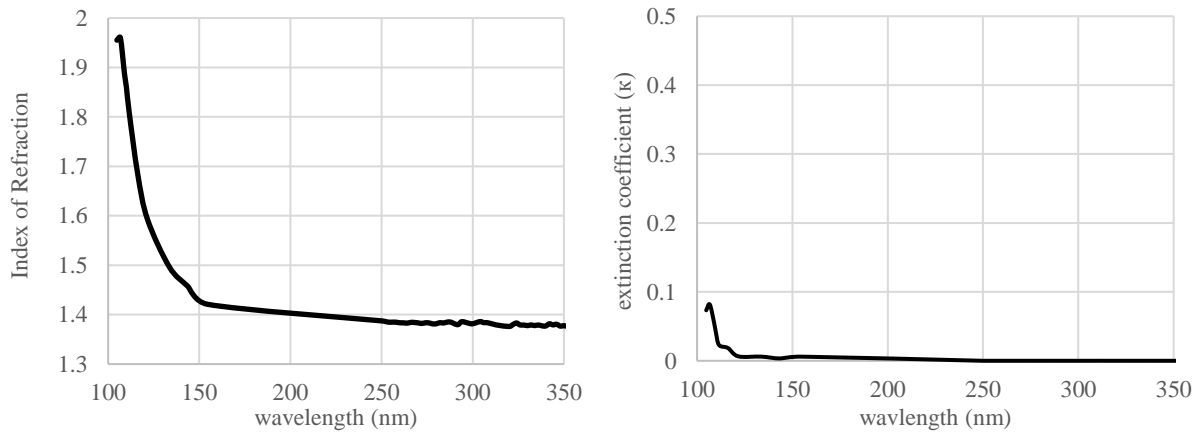


Figure 4. Index of refraction (left) and extinction coefficient (right) as a function of wavelength for AlF₃ thin films.

As seen in Figure 4, the optical properties of AlF₃ thin films show an increasing index of refraction and extinction coefficient as at the smaller FUV wavelengths. The index of refraction is between 1.4-1.38 from 200 to 350 nm while it exponentially increases at wavelengths smaller than 150 nm reaching an index of refraction of 1.96 at 107 nm. The extinction coefficient stays near zero down to 116.2 nm, then begins increasing at a higher rate nearly reaching .1 at 104.8 nm.

4.3 Design of Fabry-Perot type FUV band-pass filter

Using the optical properties in section 4.3, we are then able to design the proposed Fabry-Perot type FUV band-pass filter. The designed FUV band-pass filter using MgF_2 as the substrate, Al as the metal layer, and AlF_3 as the dielectric layer is displayed in Figure 5.

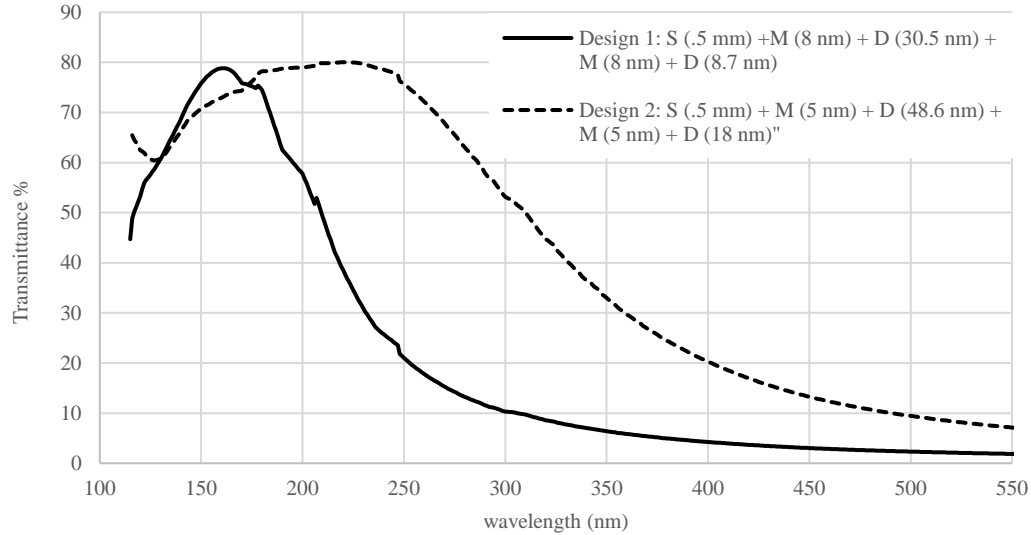


Figure 5. Four-layer Fabry-Perot FUV Filter designs consisting of an MgF_2 substrate (S), Al metal layers (M), and an AlF_3 dielectric layers (D).

Both designs peak near 80%, however, Design 1 has a narrower band-pass and enhanced visible attenuation than Design 2. Design 2 has an average transmittance near 80% from 175 nm to 250 nm while Design 1 maintains the same transmittance from 156 nm to 165 nm. The design can be modified to meet band-pass and visible photon attenuation needs. By increasing the Al layer thickness, the visible spectrum is further suppressed and the full width half maximum (FWHM) band-pass of the filter is decreased. Design 1 and 2 have a FWHM of 105 nm and 218 nm respectively. Both designs are limited by the substrate material. MgF_2 has a cut off wavelength near 115 nm causing UV absorption near that wavelength. Design 1 was modified so that the attenuation starts at wavelengths above 300 nm suppressing visible transmission to below 5%.

5. CONCLUDING REMARKS

AlF_3 is a low FUV absorbing coating that can be used in both FUV reflectors and band-pass coating design. FUV reflectors composed of Al+ AlF_3 were deposited using thermal resistive evaporation and a reflectance of more than ~90% was obtained from 120 nm to 130 nm. The AlF_3 layer in the coating design can be deposited thinner to enhance the wavelengths below 110 nm, however, the reflectance at the larger FUV wavelengths slightly decreases. AlF_3 was shown to have an index of refraction near 1.4 from 150 nm to 350 nm. The index of AlF_3 at wavelengths under 150 nm exponentially increases to a value close to 2. AlF_3 was shown to have very low absorbing properties down to 110 nm. Using the material properties derived, we were able to design FUV solar blind band-pass filters that can meet FWHM band-pass and solar suppression requirements of future UV spectrograph needs.

6. ACKNOWLEDGEMENTS

We acknowledge the NASA Goddard Space Flight Center (GSFC) thin films lab for support of this work. We also would like to thank the NASA GSFC Internal Research and Development (IRAD) Astrophysics grant for funding this work.

REFERENCES

- [1] Bolcar, M.R., Feinberg, L., France, K., Rauscher, B. J., Redding, D., Schiminovich, D., "Initial technology assessment for the Large-Aperture UV-Optical-Infrared (LUVOIR) mission concept study," Proc. SPIE 9904, Space Telescopes and Instrumentation 2016: Optical, Infrared, and Millimeter Wave, 99040J (July 29, 2016).
- [2] Bolcar, M.R. et al., "Technology development for the Advanced Technology Large Aperture Space Telescope (ATLAST) as a candidate large UV-Optical-Infrared (LUVOIR) surveyor," Proc. SPIE 9602, UV/Optical/IR Space Telescopes and Instruments: Innovative Technologies and Concepts VII, 960209 (September 22, 2015).
- [3] Tumlinson, J. et al., "Unique Astrophysics in the Lyman Ultraviolet," ArXiv e-prints , Sept. 2012.
- [4] Taubert, R. D. et al., "The Spectral Photon Flux of the Radiometric Calibration Source for the NIRSPEC Instrument of the James Webb Space Telescope," Metrologia 46, S207-S212 (2009).
- [5] F. Lei, W. Paustian, and E. Tegeler, "Determination of the spectral radiance of transfer standards in the spectral range 110 nm to 400 nm using BESSY as a primary source standard," Metrologia 32, 589–592 (1995).
- [6] Fleming, B.T. et al., "SISTINE: a pathfinder for FUV imaging spectroscopy on future NASA astrophysics missions," Proc. SPIE 9905, Space Telescopes and Instrumentation 2016: Ultraviolet to Gamma Ray, 99050A (July 11, 2016).
- [7] Macleod, H.A., [Thin-Film Optical Filters], Institute of Physics Publishing, 3rd edition, Philadelphia, Chapters 3-7, 2001.
- [8] Hass, G. "Filmed surfaces for reflecting optics," J. Opt. Soc. Am., 45, 945–52, 1955.
- [9] Canfield, L. R., Hass, G. and Waylonis, J. E., "Further studies on MgF₂-overcoated aluminium mirrors with highest reflectance in the vacuum ultraviolet," *Appl. Opt.*, **5**, 45–50, 1966.
- [10] Cox, J. T., Hass, G. and Waylonis, J. E., "Further studies on LiF overcoated aluminium mirrors with highest reflectance in the vacuum ultraviolet," *Appl. Opt.*, **7**, 1535–9, 1968.
- [11] Sommer, C., Kruger, P., and Pollmann, J., "Optical spectra of alkali-metal fluorides," Phys. Rev. B, 86 (15), 155212 (2012).
- [12] M.A. Quijada, S. Rice, and E. Mentzell, "Enhanced MgF₂ and LiF Over-coated Al Mirrors for FUV Space Astronomy," *Proc. SPIE* **8450** (2012).
- [13] Wilbrandt, S., Stenzel, O., Nakamura, H., Wulff-Molder, D., Duparré, A., and Kaiser, N., "Protected and enhanced aluminum mirrors for the VUV," *Appl. Opt.* 53, A125-A130 (2014).
- [14] Barrière, A.S. and Lachter, A., "Optical transitions in disordered thin films of the ionic compounds MgF₂ and AlF₃ as a function of their conditions of preparation," *Appl. Opt.* 16, 2865-2871 (1977).
- [15] Mu, J., Lin, P.T., Zhang, L., Michel, J., Kimerling, L.C., Jaworski, F., and Agarwal, A., "Design and fabrication of a high transmissivity metaldielectric ultraviolet band-pass filter," *Appl. Phys. Lett.* 102, 213105 (2013).
- [16] Bates, B. and Bradley, D.J., "Interference filters for the far ultraviolet," *Appl. Opt.*, 5, 971 (1966).
- [17] Hennessy, J., Jewell, A. D., Hoenk, M. E., and Nikzad, S., "Metal–dielectric filters for solar–blind silicon ultraviolet detectors," *Appl. Opt.* 54, 3507-3512 (2015).
- [18] Lallo, M.D., "Experience with the Hubble Space Telescope: 20 years of an archetype," *Opt. Eng.*, 51(1), 1–18 (2012).
- [19] Sedlmeir, F., Hauer, M., Fürst, J.U., Leuchs, G., and Schwefel, H.G.L., "Experimental characterization of an uniaxial angle cut whispering gallery mode resonator," *Opt. Express* 21, 23942–23949 (2013).

